

SUPPORTING INFORMATION APPENDIX

Supporting Information Materials and Methods

Animals

Adult sea lampreys (*Petromyzon marinus*) and catsharks (*Scyliorhynchus canicula*) were obtained from fishermen in the river Dordogne (Sainte-Terre, Gironde; France) and Mediterranean Sea (Banyuls-sur-Mer; France), respectively. Sea lampreys were maintained in river water and sacrificed either during day or at night shortly after they arrived at the laboratory. Catsharks were adapted to laboratory conditions for at least three weeks in 1 m³ aquaria in circulating filtered seawater under natural conditions of photoperiod and water temperature. Elephant sharks (*Callorhynchus milii*) were collected from Westernport Bay, Victoria, Australia, and transported to the Primary Industries Research Centre where they were euthanized by decapitation. Ratfish (*Chimaera monstrosa*) were obtained from fishermen on the northern coast of Norway or eastern coast of Spanish Catalonia; they were usually dead or died immediately upon capture. All experiments were performed according to the European Union regulations concerning the protection of experimental animals.

Tissue Processing

Tissues were removed and placed in RNA Later (Ambion, Austin, TX), stored for 24 h at 4°C and then stored at -80°C until they were processed.

RNA Extraction and cDNA synthesis for cloning

Total RNA was extracted using the Trizol method (Invitrogen; Cergy Pontoise, France). A 1 µg sample of RNA was used as a template to synthesize first strand cDNAs (SMART RACE

cDNA amplification kit: Clontech; Palo Alto, CA) according to the manufacturer's instructions.

Cloning strategies for VT- and NV-AANATs

VT-AANAT: S. canicula AANAT was cloned using degenerate primers (Table S1) based on the peptide sequences of the highly conserved motifs C and A of AANAT (1). This produced a partial sequence highly similar to the corresponding sequences of known VT-AANATs. Specific primer sets were then designed for further extension by 5',3'-rapid amplification of cDNA ends (RACE; SMART RACE cDNA amplification kit; Clontech, Mountain View, CA) and the products obtained after the 5', 3'-RACE were submitted to a second round of PCR using nested primers.

The polymerase chain reaction (PCR) was done in a total volume of 25 µl as follows: 95°C (1 min) followed by 10 cycles of denaturation at 94°C (20 sec), annealing at 42°C (1 min) and extension at 68°C (30 sec), and by another 30 cycles of denaturation at 94°C (10 sec), annealing at 37°C (1 min) and extension at 68°C (30 sec). The polymerase used was Clontech Advantage (Clontech, Mountain View, CA); template was cDNA from the selected extracts. The PCR products were resolved on an agarose gel, identified and then purified using a gel extraction kit (QIAquick Gel Extraction Kit from Qiagen; Courtaboeuf, France) and subcloned into pGEM-T Easy (Promega; Madison, WI). DH5α competent bacteria were transformed by electroporation and several positive clones were obtained; sequence was then determined (Beckman Coulter Genomics, Takeley, UK).

The gene encoding *C. milii* VT-AANAT was identified by probing (BLAST) the *C. milii* database (Elephant Shark Genome Project; ICMB, Singapore; <http://esharkgenome.imcb.a-star.edu.sg/>) with the catshark sequence obtained above. This analysis identified a sequence (AAVX01255650.1) containing the start codon and the first two exons that was then used to

design specific primers (Table S1) to clone the full *C. milii* VT-AANAT ORF from retinal cDNA, as described above.

P. marinus VT-AANAT was cloned using sequences derived from a cDNA library of the river lamprey, *Lampetra fluviatilis*, constructed in pSPORT (SuperScript Plasmid System with 'Gateway Technology for cDNA Synthesis and Cloning') following the manufacturer's instructions (Life Technologies, Grand Island, NY). Sequences cloned from this library were interrogated by BLAST alignments using known teleost VT-AANATs; this yielded two hits with high sequence identity. These clones were completely sequenced and represented overlapping fragments containing most of the open reading frame (ORF) without the 5'terminus (GenBank accession # KF290562). This sequence was used to identify homologous genomic sequences from the sea lamprey *P. marinus* (Trace Archives, http://pre.ensembl.org/Petromyzon_marinus/Info/Index). Primers were designed based on this genomic sequence to obtain an amplicon from retinal cDNA from this species containing the entire ORF (Table S1). This same amplicon was obtained from 4 different cDNA preparations synthesized in two different labs.

We interrogated the genome and transcriptome of the little skate (*Leucoraja erinacea*; <http://skatebase.org/>) using the Chimaera sequences obtained as described above. This resulted in the identification of a partial skate VT-AANAT sequence which has been deposited in the GenBank Third Party Annotation database (GenBank TPA accession # BK008791).

NV-AANAT: The NV-AANAT sequence from *C. milii* was obtained by interrogating the elephant shark genome database (<http://esharkgenome.imcb.a-star.edu.sg>) using a NV-AANAT sequence from amphioxus (GenBank accession # XP_002608038.1). This search

identified overlapping clones with a putative start codon and an intron. Primers designed against this sequence were used to amplify the full ORF from retinal cDNA (Table S1), as described above.

Primers designed against the *C. milii* sequence were used to amplify a fragment of the NV-AANAT from the ratfish *C. monstrosa*, and primers designed against this fragment were used to amplify the full ORF from retinal cDNA (Table S1), as described above.

In silico attempts to identify NV-AANAT in the lamprey genome (see above) by BLAST search using NV-AANAT sequences obtained from amphioxus or elephant shark as queries were unsuccessful; in addition, PCR (using several sets of degenerate primers) also failed to identify a lamprey NV-AANAT. We also interrogated the genome and transcriptome of the little skate (*Leucoraja erinacea*) and the transcriptome of the catshark (*S. canicula*), both available at <http://skatebase.org/>, using the Chimaera sequences obtained as described above. This analysis resulted in the identification of a full-length skate NV-AANAT which has been deposited in the GenBank Third Party Annotation database (GenBank TPA accession # BK008792). In contrast, NV-AANAT sequence was not identified in the catshark transcriptome.

RT-PCR to Determine Tissue Distribution

RT-PCR identification of VT-AANAT in tissue extracts from lamprey and catshark was performed using primers described in Table S1.

A 1 µg sample of RNA extracted (see above) from different tissues was incubated 20 min at 37°C with 1 unit of DNase I (Roche Diagnostics, Meylan, France). Following DNase inactivation (10 min at 65°C), RNA was reverse transcribed using Powerscript reverse transcriptase (Clontech, Mountain View, CA). PCR amplification of the generated cDNAs was

done using specific forward (F) and reverse (R) primers designed from the cloned sequence (Table S1) and the following conditions: 95°C (1 min), 30 cycles of 94°C (20 sec), 60.5°C (1 min), 68°C (1 min), and terminated with 7 min at 68°C. For controls, template cDNA was replaced by either water or RNA that was not reverse transcribed. The PCR products were separated and detected in an agarose gel with DNA size markers (DNA/Hinf I or 1 kb DNA ladder markers; PromegaFr, Charbonnières, France). Fragments of the expected size were extracted, subcloned into pGEM-T Easy and sequenced as indicated above.

Preparation of GST-AANAT Fusion Proteins

The coding regions of VT- and NV-AANATs were amplified by PCR using pairs of specific primers (Table S2) that contained enzyme restriction sites. The AANAT PCR products were subcloned into pGEM-T Easy and sequenced. Each positive clone was digested with BamHI and NotI and ligated into a BamHI/NotI-cut pGEX4T1 vector (Novagen, EMD Chemicals Inc, Philadelphia, PA). This construct generated an AANAT fused to glutathione S-transferase (GST). The clones were transformed into BL21 *Escherichia coli* and bacteria were grown at 37°C until they reached an O.D. of 0.6. Recombinant protein production was induced with 0.2 mM isopropylthiogalactopyranoside (IPTG) at the required duration and temperature (*C. milii* NV-AANAT: 15 h, 20°C; *C. milii* VT-AANAT: 5 h, 20°C; *P. marinus* VT-AANAT: 5 h, 21°C; *S. canicula* VT-AANAT: 5 h, 37°C). Subsequent steps were carried out at 4°C. The bacteria were pelleted, suspended in 25 ml of buffer (Tris 50 mM pH 8, NaCl 150 mM containing phenylmethylsulfonylfluoride 0.5 mM, benzamidine 1 mM, leupeptine 4 µM, dithiothreitol 1 mM, ethylene diamine tetraacetic acid [EDTA] 0.5 mM, ethylene glycol tetraacetic acid [EGTA] 0.5 mM) per 500 ml growth medium, and sonicated. To this mixture was added Triton X100 (1% final) and Tween 20 (0.1% final); it was then centrifuged (30,000

g, 4°C) for 15 min. The supernatant was mixed with Glutathione Sepharose 4B beads (GE Healthcare, Buckinghamshire, UK). The beads were washed 3 times with Tris buffered saline (TBS, pH 8) containing 1% Triton X100 and 0.1% Tween 20 and once with TBS, pH 8. The GST-AANAT fusion protein was eluted from the beads with 1 ml of buffer containing 10 mM glutathione in 50 mM Tris, pH 8. The recombinant protein was stored in aliquots at -80°C. Protein amount was quantified using the BioRad Protein Assay Dye Reagent (BioRad, Marnes-la-Coquette, France) with bovine serum albumin as standard.

Enzyme Activity Assays

AANAT enzyme activity was measured using the colorimetric assay (2) for the recombinant proteins and the radioactive assay (3) for tissue extracts.

Colorimetric assay: Typically, reactions were performed in 96 well plates (Greiner BioOne, Monroe, NC); each well contained a reaction volume of 100 µl, including 5 µl of enzyme solution, 70 µl of phosphate assay buffer (0.1 M, pH 6.8) containing (final concentrations): AcCoA 0.5 mM, EDTA 2 mM, BSA 0.05 mg/ml, and 25 µl of buffer or substrate at the indicated concentrations. Other conditions are detailed in the Results section and figure legends. The reaction was terminated by the addition of 150 µl stop solution (0.2 M phosphate buffer pH 6.1, containing 1 mM DTNB, 10 mM EDTA, and 3 M guanidine hydrochloride) and the optical density in each well was measured at 405 nm after 5 min of incubation at room temperature. Kinetic constants were calculated as indicated below. Controls were run using a reaction medium that contained no or heat-treated (65°C, 5 min) enzyme, or coenzyme A-S-acetyltryptamine (CoA-S-AcT; 100 µM) (NIMH Chemical Synthesis and Drug Supply Program, <http://nimh-repository.rti.org/>); CoA-S-AcT is an AANAT bisubstrate inhibitor (4).

Radiometric assay: The organs and tissues were homogenized (sonication) in 100 μ l of phosphate buffer (0.1 M, pH 6.8) and centrifuged at 4°C for 1 min at 13,400 g. Proteins in the supernatant were quantified as indicated above for the preparation of the GST-fusion proteins. Typically, the assay was performed under the same conditions as for the colorimetric assay using 50 μ l of supernatant and [³H]-AcCoA (GE Healthcare, Buckinghamshire, UK) at a final specific activity of 4 mCi/mmol. The reaction was stopped by the addition of 1 ml chloroform. Acetylated products were extracted, and radioactivity was counted, as described (5).

Modeling

Three-dimensional models of the elephant shark VT- and NV-AANAT were built based on homology to the structure of ovine AANAT determined by X-ray crystallography (PDB code: 1cjw) using the MOE software package (Chemical Computing Group, Inc.) following the procedure described in its homology modeling tutorial. The models were rendered using the programs MolScript(6) and Raster3D (7).

Computational Sequence Analysis

The BLASTP program (8) was used for sequence similarity searches against the NCBI Non-Redundant database. Protein sequence alignments were produced using the MAFFT program (9). Large-scale (>100 sequences) phylogenetic analysis was performed using the FastTree program (10). Evolutionary model selection was performed using the ProtTest program (11). Detailed phylogenetic analysis was performed using the RAxML program (12) with the LG evolutionary model and gamma-distributed site rates. Divergence times (expert estimates) were obtained from the TimeTree.org website (13). The large-scale and

constrained maximum-likelihood phylogenetic trees (Figs. S5 and 4B, respectively) are available in Newick format at ftp://ftp.ncbi.nih.gov/pub/wolf/_suppl/aanat/.

Evolutionary rates were calculated as the number of substitutions per site per million years, obtained by dividing the branch length in substitutions per site estimated with RAxML by the duration of the respective time interval obtained from TimeTree (14).

***In situ* Hybridization**

In situ hybridization (ISH) was performed as indicated elsewhere (15) with slight modifications. Tissues were obtained from lampreys (*P. marinus*) and catsharks (*S. canicula*). After sacrifice, the organs were rapidly removed, fixed in freshly prepared 4% paraformaldehyde in phosphate buffer (0.1 M, pH 7.4) overnight at 4°C, dehydrated and embedded in paraffin wax (16). Sections (10 µm) were mounted on silane-coated slides and were deparaffinized for the ISH. The digoxigenin-labeled sense and anti-sense riboprobes were prepared using a commercially available kit (Roche Diagnostics; Meylan, France). The catshark VT-AANAT probe was generated using a 1100 bp cDNA fragment starting from bp 630 of the sequence to its end. The lamprey VT-AANAT probe was generated using a 357 bp fragment starting at bp 15 from the start codon. Hybridization was done using a probe concentration of 1 µg/ml and digoxigenin was immuno-detected using a commercially available kit (Roche Diagnostics, Meylan, France).

Chemicals

Unless otherwise indicated in the text, all chemicals were from Sigma-Aldrich (Saint-Quentin Fallavier, France).

Table S1

Primers list

<i>S. canicula</i> VT-AANAT	Degenerate primers for cloning	
	forward	gtttgaratcgagagagargc
	reverse	gatggagccyttgccctgctg
	Specific primers for 5',3'-RACE	
	5' extension	gaacggccaagacatggatgtggacagtgg
	5' nested	ggtcagagcatcctgtgacagttgtcctt
	3' extension	ggagagtgtcctttacacatggatgaagtg
	3' nested	tgtgtcctgagctatctcttggtggttg
	Specific primers for RT-PCR from the different tissue extracts	
	forward	aagaggaactggtcagaagc
reverse	aggtgaactccagtccattc	
<i>C. milii</i> VT-AANAT	Specific primers for cloning	
	forward	atggccacagcgcctcctctcccttc
	reverse	ttagcagccgctattctgagcaggaagc
	Specific primers for 3'-RACE	
	3' extension	tgcacatggatgaagtgagacactttctcg
	3' nested	gctggtttgaggaggcagactagtagcct
	Specific primers for RT-PCR from the different tissue extracts	
	forward	gcgagttcagaaacctgagtct
reverse	ctatttctgagcaggaagctc	
<i>P. marinus</i> VT-AANAT	Specific primers for cloning	
	forward	gctggatcccacgaacatcaagaagaag
	reverse	tcaccaaccgctattcctccgagcttc
	Specific primers for RT-PCR from the different tissue extracts	
	forward	aagaggaggtggagacctta
	reverse	ctctcgatttcaagacgct
<i>P. marinus</i> β-Actin	Degenerate primers for RT-PCR from the different tissue extracts	
	forward	ctggagaagagctaygagctg
	reverse	gtacatggtgtaccdccaga

<i>C. milii</i> NV-AANAT	Specific primers for cloning	
	forward	atgcaaacaggggcagagat
	reverse	tcaacagcgctccatggtgag
	Specific primers for RT-PCR from the different tissue extracts	
	forward	atgtgtactcagcctgggagtt
reverse	tgctgaatccagctttgatgta	

<i>C. milii</i> β-Actin	Specific primers for RT-PCR from the different tissue extracts	
	forward	aagacatcagggtgatggttg
	reverse	ggagcaatgatcttgatcttcatgg

<i>C. monstrosa</i> NV-AANAT	Specific primers for cloning	
	forward 1	aactcatcggctttgtgtg
	reverse 1	gtactgggtgctcaggagac
	forward 2	tgagctcagagcgccaag
	reverse 2	ctcagtgtgggttcatcaac
	Specific primers for 5',3'-RACE	
	5' extension	aggtcacgtccacacacag
	5' nested	cttcatggaggcttcagtcag
	3' extension	cactctgtgtgtggacgtg
	3' nested	gatatgtctcctgagccacca

Table S2

Primers used for the preparation of GST-AANAT fusion proteins

<i>P. marinus</i> VT-AANAT	forward	gcggatggatccatgtcccacgaaca
	reverse	agccgcgccgcagaccaaccgctat
<i>S. canicula</i> VT-AANAT	forward	gctgagggatccatgacagcaagcag
	reverse	catgacgcgccgcttagcagccactgt
<i>C. milii</i> VT-AANAT	forward	ggatccatggccacagcgagcgctc
	reverse	gcggccgctatgcagccgctattct
<i>C. milii</i> NV-AANAT	forward	ggatccatgcaaacaggggcagagat
	reverse	gcggccgctatacagcgtccatgtt

Table S3**Rates of AANAT evolution**

Average rates (substitutions per site per million years) were calculated by dividing the total length of the subtrees by the sum of the times along the corresponding branches as shown in Table S4.

Subtree	Rate	Relative Rate
NV-type	0.00091	x1
VT-type	0.00047	x0.5
VT-type base	0.01104	X12.1

Table S4 Calculation of estimated evolutionary rates for VT- and NV-AANAT. Blue: metazoan NV-AANAT; magenta: VT-AANAT; red: VT-AANAT base branch. See the Methods section above for details. These data are shown graphically in Figure S6.

Branch	Branch start, MYA	Branch end, MYA	Branch time, MY	Branch length, subs/site	Evolution rate, x0.001 subs/site/MY
Homo/Pan -> Homo	6.2	0.0	6.2	0.0058	0.937
Homo/Pan -> Pan	6.2	0.0	6.2	0.0117	1.893
Simiiformes -> Homo/Pan	29.6	6.2	23.4	0.0122	0.521
Simiiformes -> Macaca	29.6	0.0	29.6	0.0420	1.421
Euarchontoglires -> Simiiformes	91.0	29.6	61.4	0.0777	1.266
Euarchontoglires -> Mus	91.0	0.0	91.0	0.0210	0.231
Eutheria -> Euarchontoglires	97.4	91.0	6.4	0.0534	8.339
Eutheria -> Bos	97.4	0.0	97.4	0.1345	1.381
Mammalia -> Eutheria	176.1	97.4	78.7	0.0747	0.949
Mammalia -> Monodelphis	176.1	0.0	176.1	0.1027	0.583
Amniota -> Mammalia	324.5	176.1	148.4	0.1388	0.935
Amniota -> Anolis	324.5	0.0	324.5	0.0278	0.086
Tetrapoda -> Amniota	361.2	324.5	36.7	0.1388	3.781
Tetrapoda -> Xenopus	361.2	0.0	361.2	0.0976	0.270
Sarcopterygii -> Tetrapoda	430.0	361.2	68.8	0.0162	0.236
Sarcopterygii -> Latimeria	430.0	0.0	430.0	0.0538	0.125
Teleostomi -> Sarcopterygii	454.6	430.0	24.6	0.0000	0.000
Euteleostei -> Esox	264.0	0.0	264.0	0.1342	0.508
Euteleostei -> Oncorhynchus	264.0	0.0	264.0	0.1195	0.453
Actinopterygii -> Euteleostei	307.0	264.0	43.0	0.0133	0.309
Actinopterygii -> Danio	307.0	0.0	307.0	0.0650	0.212
Teleostomi -> Actinopterygii	454.6	307.0	147.6	0.0276	0.187
Gnathostomata -> Teleostomi	526.5	454.6	71.9	0.1258	1.749
Chondrichthyes -> Scyliorhinus	471.0	0.0	471.0	0.0521	0.111
Chondrichthyes -> Callorhynchus	471.0	0.0	471.0	0.0356	0.076
Gnathostomata -> Chondrichthyes	652.0	471.0	181.0	0.1525	0.843
Vertebrata -> Petromyzon	652.0	0.0	652.0	0.5416	0.831
VT base	797.0	652.0	145.0	1.6011	11.042
Chimaeriformes -> Callorhynchus	220.0	0.0	220.0	0.0788	0.358
Chimaeriformes -> Chimaera	220.0	0.0	220.0	0.0716	0.325
Chondrichthyes -> Chimaeriformes	471.0	220.0	251.0	0.3548	1.414
Chondrichthyes -> Leucoraja	471.0	0.0	471.0	0.3458	0.734
Chordata -> Vertebrata	797.0	471.0	326.0	0.2715	0.833
Chordata -> Branchiostoma floridae	797.0	0.0	797.0	0.5476	0.687
Bilateria -> Chordata	910.0	797.0	113.0	0.0000	0.000
Bilateria -> Capitella	910.0	0.0	910.0	0.9528	1.047
Fungi/Metazoa -> Bilateria	1368.0	910.0	458.0	0.8227	1.796

B. Alignment of Chondrichthyes and amphioxus NV-AANATs

```

C. milii           MQTGAEIRWLSG-GDVYSAWELETAGYPPEEAASLEILQYRQREAGELFPGYYINTKLI 59
C. monstrosa      MLTGAEIRWLSE-GDVRSAWLETAGYPPEEAASLESLRYRQREAGELFQGYINTKLI 59
L. erinacea       MQPEGEIRTLA-EEVAPALALEVSAFPPEEAASLRQLQYRQREVGNFFQGNFINGKLV 59
B. lanceolatum    -MAEGNVRPLQCGEEVEQASILESAGYPADEAASLETLQARHTAESRLFIGYFENEKLL 59
                  . . : * * . : * * ** . : * . : * * * . * : * : . : * * : * * * *

```

```

C. milii           FVCGTRSFADHLTDASMKVHEAGGPTVCIHSVCVDVTWRRKGIALSLLQHYVRDISQN 119
C. monstrosa      FVCGTRCFADYLTEASMKVHEPGGPTVCIHSVCVDVTWRRKGVALSLLQHYIRAIQN 119
L. erinacea       FICGTRSVADHITQRSMEVHESAGTTICHSVCVDQAWRRRGIALSLLRHFVEVVRHS 119
B. lanceolatum    FVCATSTDADRLTEESMHTHIPHGETICHSVCVDQSVQRQGIATKLLKEFVHNKGS 119
                  * : * . * ** : * : * * . * . * * : * * * * * : * : * : * . * : * : * .

```

A

```

C. milii           DVHQICLLSHQYLLPLYIKAGFSNIGLSSVHGPDKWYECILNMERC 166
C. monstrosa      DVQRICLLSHQSLLPLYTKAGFNINIGFSVAVHGPDKWYECILNMERC 166
L. erinacea       TARRICLICHLQLLPLYTKAGFTLLGPSTVTHGPDWYECTMDLN-- 164
B. lanceolatum    DAKRICLICHEYLIPLYTKAGFVLVGLSEVHVGKEPWyDCVMEL--- 163
                  . : * * : * * * * * * * * * * * * * * * * * * * * * * * * * * *

```

B

C. Alignment of *C. milii* NV/VT AANAT

```

NV -----MQTGAEIRWLSGGDVYSAWELETAGYPPEE 30
VT MATAIASSPFLKPFALRYSVGSSPGRQRRLTPASEFRNLSLQDAISVFEIEREAFISVS 60
                  . . : * * * * . * . * : * * * * . : * .

```

C

```

NV ---AASLEILQYRQREAGELFPGYYINTKLI GFVCGTRSFADHLTDASMKVHEAGGPTVC 87
VT GECPLHMDEVRFLELCPLESLGWFEGRVAFVIGSGWDKEKLSQDALTIHVPDAPT VH 120
_ . : : : * * * * : * : * * * : * : * : * : * : * : * : * *

```

D

```

NV IHSVCVDVTWRRKGIALSLLQHYVRDISQNQTDVHQICLLSHQYLLPLYIKAGFSNIGLS 147
VT IHVLAVHHKCRQGGKSIILWRYLQYLR-CLAMVKRAVLMCEDFLIPFYQKAGFKDIGPS 179
* * : * . * . * : * : * * : * : * : * : * : * : * : * : * : * : *

```

A

B

```

NV SVVHGPDKWYECILNMERC----- 166
VT GVAVGPLTFTEMEYTLGGGAYLRRNSGC 206
* . * * . : * . :

```

Legend of Figure S1. VT- and NV-AANAT alignments.

A: Alignment of *P. marinus* (KF246473), *S. canicula* (EU378921), *L. erinacea* (reconstructed from LSb2-contigs 244146, 28819, 3043531 and LS-transcriptB2-contig 50898; skate base project), *C. milii* (KF246475), *E. lucius* AANAT1a (AF034081.1), and *O. aries* (U29663.1) VT-AANAT. Conservation is high in the AcCoA (A and B) and substrate (C and D) binding domains (overlined). All the enzymes show the putative PKA phosphorylation sites (bold red) characteristic of all VT-AANAT cloned to date. Conserved residues thought to be important for the substrate and co-substrate binding and/or catalytic activity are in bold violet and green. In bold blue are putative casein kinase 2 phosphorylation sites. For more details see (17-25). Asterisk: fully conserved residue; column: groups of strongly similar properties; period: groups of weakly similar properties

B: Alignment of the Chondrichthyes *C. milii* (KF246476) and *C. monstrosa* (KF246474) NV-AANAT with the little skate NV-AANAT (*L. erinacea* genome project (26, 27) Genome Contigs 1750401 and 2695118) and amphioxus NV-AANAT β form (*B. floridae* genome V1.0, scaffold_54|2461188|2461676) (28, 29). High amino-acid identity is found in the AcCoA binding motifs A and B. Important residues are colored as in panel **A**.

C: Alignment of NV- and VT-AANAT from *C. milii* (KF246475 and KF246476, respectively). Important residues are colored as in panel **A**.

Figure S2

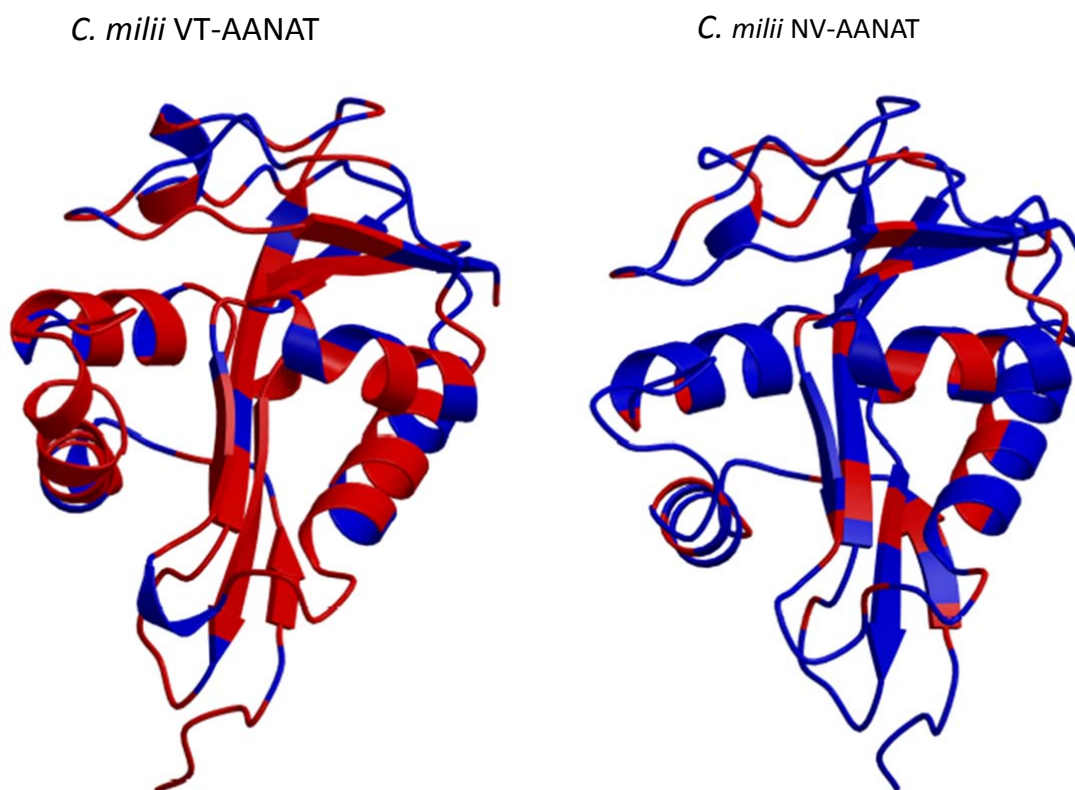
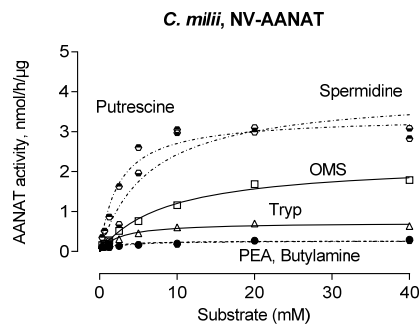
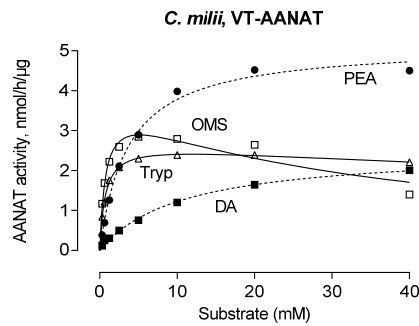
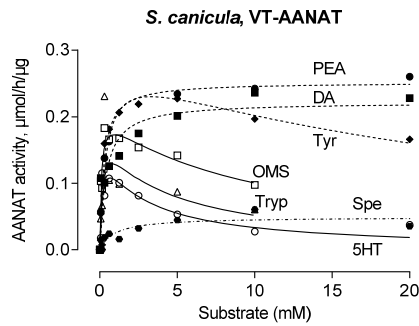
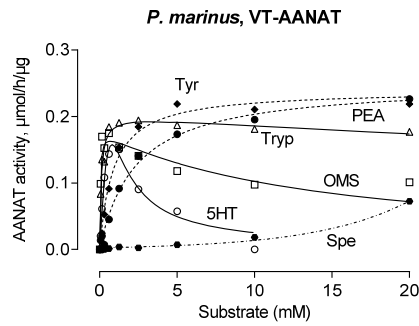


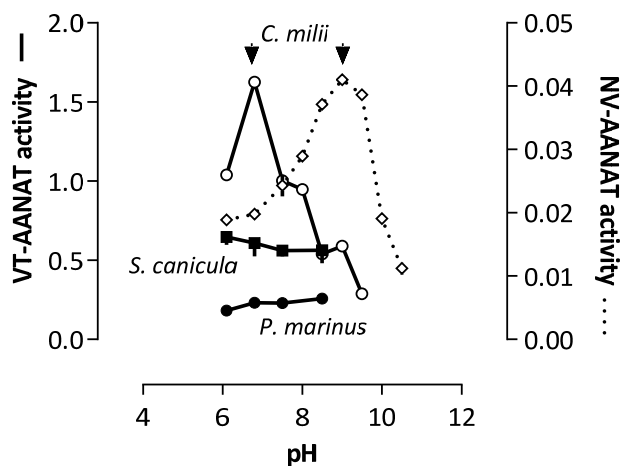
Figure S2. Three dimensional models of *C.milii* VT- and NV-AANAT. Structures were modeled using the crystal structure of the VT-AANAT from *Ovis aries* as outlined above. Residues identical to those in the ovine template are colored red; all others are colored blue. Each model is oriented to show the conserved (red) residues that span the beta sheet. The conserved inner face of a helix is also evident in NV-AANAT (at 4 o'clock).



AANAT activity of recombinant enzymes as a function of substrate concentration

5HT: serotonin; DA: dopamine; OMS: O-methylserotonin; PEA: phenylethylamine; Spe: spermidine; Tryp: tryptamine; Tyr: tyramine.

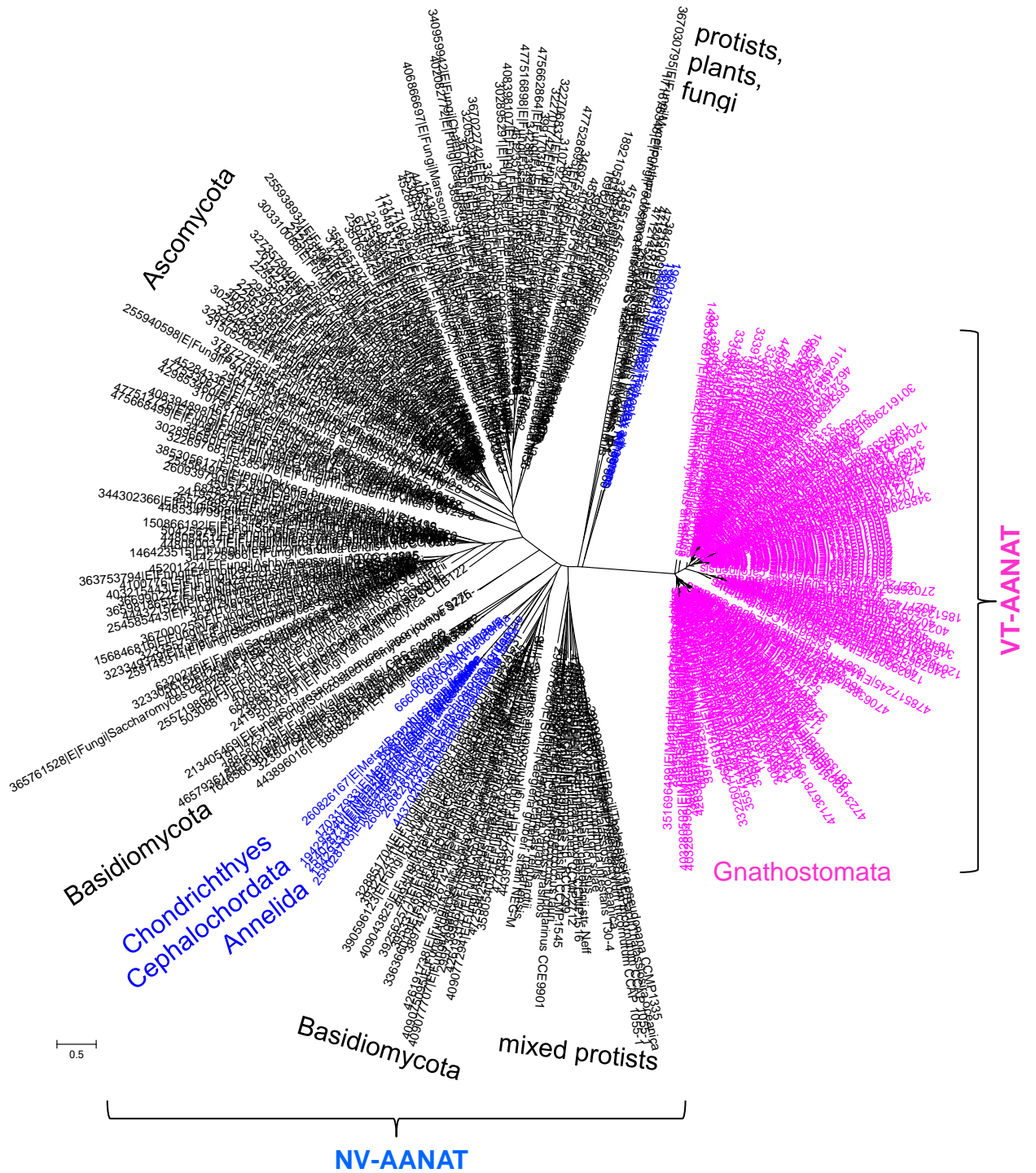
Figure S4



Activity of recombinant VT- and NV-AANATs as a function of pH

VT-AANAT (left ordinates) and NV-AANAT (right ordinates) activity were measured at 37°C as indicated in SI Appendix Materials and Methods, using phosphate buffer at different pH (abscissa), and AcCoA at the EC₅₀ concentration (1 mM for VT-AANAT, and 0.1 mM for NV-AANAT). The substrates were phenylethylamine (10 mM) for *C. milii* VT- and NV-AANAT, and tryptamine (10 mM) for *P. marinus* and *S. canicula* VT-AANAT. Activity is in $\mu\text{mol/h}/\mu\text{g}$ enzyme (mean \pm SEM, n = 3; small error bars may be masked by the plot).

Figure S5. Maximum likelihood phylogenetic tree of VT- and NV-AANATs



Legend of Figure S5. Maximum likelihood phylogenetic tree of VT- and NV-AANATs.

Seed AANAT sequences were used as queries in a BLAST search against the non-redundant protein database at NCBI (nr, e-value 0.1). The sequences found in this search were clustered (blastclust, 75% identity, 75% length coverage) and representatives of each cluster were used as queries for another round of BLAST search against nr (e-value 1e-6). Eukaryotic hits were pooled together and aligned to the manually curated alignment of the seed sequences using MAFFT. A preliminary phylogenetic tree was reconstructed using FastTree (WAG evolutionary model); a subtree including seed sequences and their immediate relatives (362 sequences) was extracted. These sequences were re-aligned to the alignment of the seed sequences using MAFFT; another tree (shown here) was reconstructed using FastTree (WAG evolutionary model). Details of tree and the included sequences can be found at `aanat.362.tre` at ftp://ftp.ncbi.nih.gov/pub/wolf/_suppl/aanat/). Black: non-metazoan NV-AANAT; blue: metazoan NV-AANAT; magenta: VT-AANAT; red: VT-AANAT base branch. The scale bar indicates the number of substitutions per site.

Figure S6

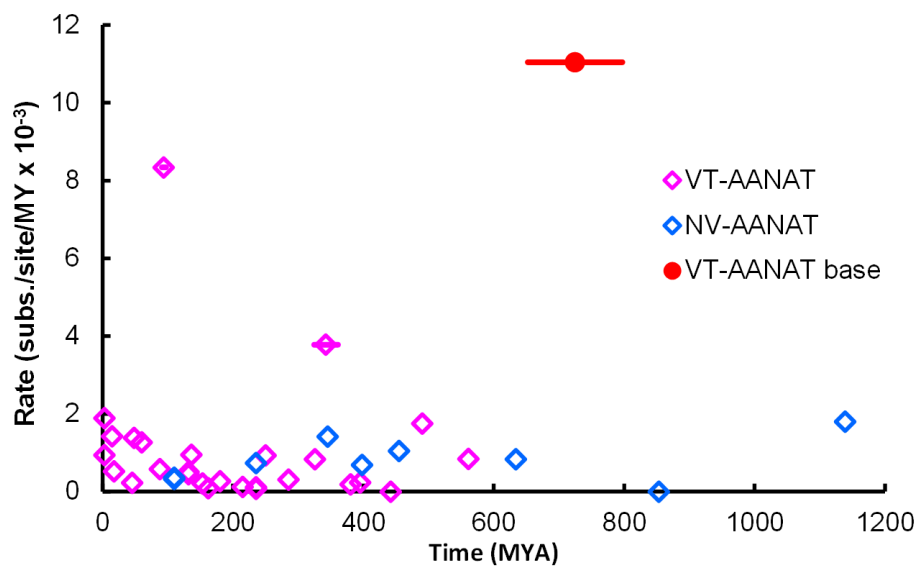


Figure S6. Estimated evolution rates of VT- and NV-AANAT. Graphed from the data given in Table S4. Blue: – metazoan NV-AANAT; magenta: – VT-AANAT; red: – VT-AANAT base branch. Coordinates on the x-axis show the middle of the corresponding branch. For the three fastest-evolving branches (Eutheria-Euarchontoglires, Tetrapoda-Amniota and VT base) the entire extent of the branch is represented with a horizontal bar.

Supporting Information References

1. Klein DC, *et al.* (1997) The melatonin rhythm-generating enzyme: molecular regulation of serotonin *N*-acetyltransferase in the pineal gland. *Recent Prog Hormone Res* 52:307-357.
2. De Angelis J, Gastel J, Klein DC, & Cole PA (1998) Kinetic analysis of the catalytic mechanism of serotonin *N*-acetyltransferase (EC 2.3.1.87). *The Journal of biological chemistry* 273(5):3045-3050.
3. Benyassi A, Schwartz C, Coon SL, Klein DC, & Falcon J (2000) Melatonin synthesis: arylalkylamine *N*-acetyltransferases in trout retina and pineal organ are different. *Neuroreport* 11(2):255-258.
4. Khalil EM & Cole PA (1998) A potent inhibitor of the melatonin rhythm enzyme. *J Amer Chem Soc* 120(24):6195-6196.
5. Falcón J, Bolliet V, & Collin JP (1996) Partial characterization of serotonin *N*-acetyltransferases from northern pike (*Esox lucius*, L.) pineal organ and retina: effects of temperature. *Pflugers Arch* 432(3):386-393.
6. Kraulis PJ (1991) Molscript - a Program to Produce Both Detailed and Schematic Plots of Protein Structures. *J Appl Crystallogr* 24:946-950.
7. Merritt EA & Bacon DJ (1997) Raster3D: photorealistic molecular graphics. *Methods Enzymol* 277:505-524.
8. Altschul SF, *et al.* (1997) Gapped BLAST and PSI-BLAST: a new generation of protein database search programs. *Nucleic Acids Res* 25(17):3389-3402.
9. Katoh K & Standley DM (2013) MAFFT multiple sequence alignment software version 7: improvements in performance and usability. *Mol Biol Evol* 30(4):772-780.
10. Price MN, Dehal PS, & Arkin AP (2010) FastTree 2--approximately maximum-likelihood trees for large alignments. *PLoS One* 5(3):e9490.
11. Darriba D, Taboada GL, Doallo R, & Posada D (2011) ProtTest 3: fast selection of best-fit models of protein evolution. *Bioinformatics* 27(8):1164-1165.
12. Stamatakis A, Ludwig T, & Meier H (2005) RAxML-III: a fast program for maximum likelihood-based inference of large phylogenetic trees. *Bioinformatics* 21(4):456-463.
13. Hedges SB, Dudley J, & Kumar S (2006) TimeTree: a public knowledge-base of divergence times among organisms. *Bioinformatics* 22(23):2971-2972.
14. Kumar S & Hedges SB (2011) TimeTree2: species divergence times on the iPhone. *Bioinformatics* 27(14):2023-2024.
15. Besseau L, *et al.* (2006) Melatonin pathway: breaking the 'high-at-night' rule in trout retina. *Exp Eye Res* 82(4):620-627.
16. Martoja R & Martoja M (1967) *Initiation aux techniques de l'histologie animale* (Masson, Paris) p 345.
17. Cazaméa-Catalan D, *et al.* (2012) Functional diversity of Teleost arylalkylamine *N*-acetyltransferase-2: is the *timezyme* evolution driven by habitat temperature? *Molec Ecol* 21(20):5027-5041.
18. Cazaméa-Catalan D, *et al.* (2013) Unique arylalkylamine *N*-acetyltransferase-2 polymorphism in salmonids and profound variations in thermal stability and catalytic efficiency conferred by two residues. *J Exp Biol* 216:1938-1948.
19. Hickman AB, Klein DC, & Dyda F (1999) Melatonin biosynthesis: The structure of serotonin *N*-acetyltransferase at 2.5 angström resolution suggests a catalytic mechanism. *Mol Cell* 3(1):23-32.
20. Hickman AB, Namboodiri MAA, Klein DC, & Dyda F (1999) The structural basis of ordered substrate binding by serotonin *N*-acetyltransferase: Enzyme complex at 1.8 angström resolution with a bisubstrate analog. *Cell* 97(3):361-369.

21. Obsil T, Ghirlando R, Klein DC, Ganguly S, & Dyda F (2001) Crystal structure of the 14-3-3 zeta : serotonin *N*-acetyltransferase complex: A role for scaffolding in enzyme regulation. *Cell* 105(2):257-267.
22. Zilberman-Peled B, Bransburg-Zabary S, Klein DC, & Gothilf Y (2011) Molecular evolution of multiple arylalkylamine *N*-acetyltransferase (AANAT) in fish. *Mar Drugs* 9(5):906-921.
23. Wolf E, De Angelis J, Khalil EM, Cole PA, & Burley SK (2002) X-ray crystallographic studies of serotonin *N*-acetyltransferase catalysis and inhibition. *J Mol Biol* 317(2):215-224.
24. Pavlicek J, *et al.* (2008) Evidence that proline focuses movement of the floppy loop of arylalkylamine *N*-acetyltransferase (EC 2.3.1.87). *J Biol Chem* 283(21):14552-14558.
25. Dyda F, Klein DC, & Hickman AB (2000) GCN5-related *N*-acetyltransferases: A structural overview. *Ann Rev Biophys Biomol Struct* 29:81-103.
26. Wang Q, *et al.* (2012) Community annotation and bioinformatics workforce development in concert--Little Skate Genome Annotation Workshops and Jamborees. *J Biol Data Base Cur* 2012:bar064.
27. King BL, Gillis JA, Carlisle HR, & Dahn RD (2011) A natural deletion of the HoxC cluster in elasmobranch fishes. *Science* 334(6062):1517.
28. Pavlicek J, *et al.* (2010) Evolution of AANAT: expansion of the gene family in the cephalochordate amphioxus. *BMC evolutionary biology* 10:154.
29. Putnam NH, *et al.* (2008) The amphioxus genome and the evolution of the chordate karyotype. *Nature* 453(7198):1064-1071.